

SUPPORTING INFORMATION

Carbide-derived carbon beads with tunable nanopores from continuously produced polysilsesquioxanes for supercapacitor electrodes

Benjamin Krüner,^{1,2,†} Christina Odenwald,^{3,†} Aura Tolosa,^{1,2} Anna Schreiber,¹
Mesut Aslan,¹ Guido Kickelbick,^{3,*} and Volker Presser^{1,2,*}

¹ INM - Leibniz Institute for New Materials, 66123 Saarbrücken, Germany

² Department of Materials Science and Engineering, Saarland University, 66123 Saarbrücken, Germany

³ Inorganic Solid State Chemistry, Saarland University, 66123 Saarbrücken, Germany

[†] these authors contributed equally

* Corresponding authors' eMails:

guido.kickelbick@uni-saarland.de (G. Kickelbick); volker.presser@leibniz-inm.de (V. Presser)

Table S1: Properties of the PTFE-bound electrodes.

	Electrode density ($\text{mg}\cdot\text{cm}^{-3}$)	Active mass of one electrode (mg)	Electrode disc diameter (mm)	Electrode thickness (μm)
1 M TEA-BF₄ in acetonitrile				
Vi-SiOC-CDC	197	1.15	8	122
Ph _{0.25} Vi _{0.75} -SiOC-CDC	372	2.33	8	131
Ph _{0.5} Vi _{0.5} -SiOC-CDC	452	2.51	8	116
Ph _{0.75} Vi _{0.25} -SiOC-CDC	438	2.41	8	115
AC	435	2.27	8	109
Aqueous 1 M Na₂SO₄				
Vi-SiOC-CDC	206	1.47	8	150
Ph _{0.25} Vi _{0.75} -SiOC-CDC	377	2.24	8	124
Ph _{0.5} Vi _{0.5} -SiOC-CDC	450	2.51	8	117
Ph _{0.75} Vi _{0.25} -SiOC-CDC	432	2.44	8	118

Table S2: Porosity of the Vi-SiOC-CDC electrodes measured with nitrogen gas sorption.

	SSA _{DFT} ($\text{m}^2\cdot\text{g}^{-1}$)	SSA _{DFT} loss after voltage floating (%)	SSA _{BET} ($\text{m}^2\cdot\text{g}^{-1}$)	Total pore volume ($\text{cm}^3\cdot\text{g}^{-1}$)	Total pore volume loss after voltage floating (%)	Average pore size (nm)
Vi-SiOC-CDC initial electrode	1756	-	2287	1.83	-	2.5
Vi-SiOC-CDC negative electrode	980	44	1515	1.23	34	2.6
Vi-SiOC-CDC positive electrode	897	49	1403	1.19	35	2.8

Table S3: EDX element analysis of Vinyl-SiOC-CDC electrodes before the electrochemical testing and after the voltage floating at 1.4 V for 100 h in aqueous 1 M Na₂SO₄. Values below the detection limit are denoted n.d. (not detected).

	C (mass%)	O (mass%)	Si (mass%)	F (mass%)	Na (mass%)	S (mass%)	Cl (mass%)
Vi-SiOC-CDC initial electrode	89.5±0.6	4.1±0.3	3.5±0.3	2.9±0.3	n.d.	n.d.	n.d.
Vi-SiOC-CDC positive electrode	81.3±1.3	7.4±1.0	1.6±0.3	3.5±1.1	4.6±0.6	0.7±0.2	0.9±0.2
Vi-SiOC-CDC negative electrode	81.3±0.5	4.4±0.8	2.2±0.1	6.6±1.6	4.4±0.4	0.5±0.1	0.7±0.1

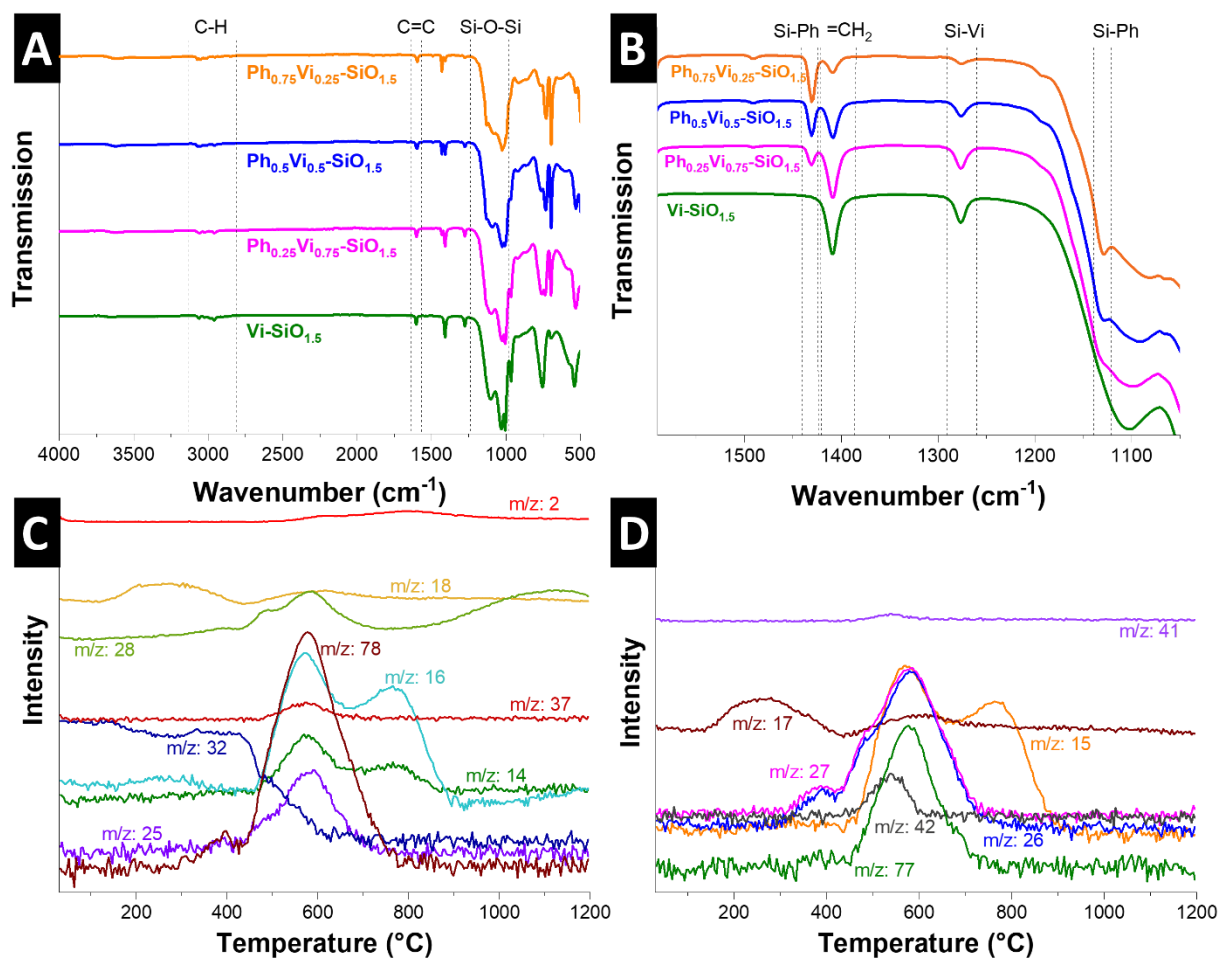


Figure S1: Overview of the FT-IR spectra of the four polymer beads (A) and detailed spectra in the range of 1000-1600 cm^{-1} (B). The corresponding mass spectra of $\text{Ph}_{0.5}\text{Vi}_{0.5}\text{-SiO}_{1.5}$ to the thermogram shown in Fig. 2D of relevant evolving groups (C) and (D).

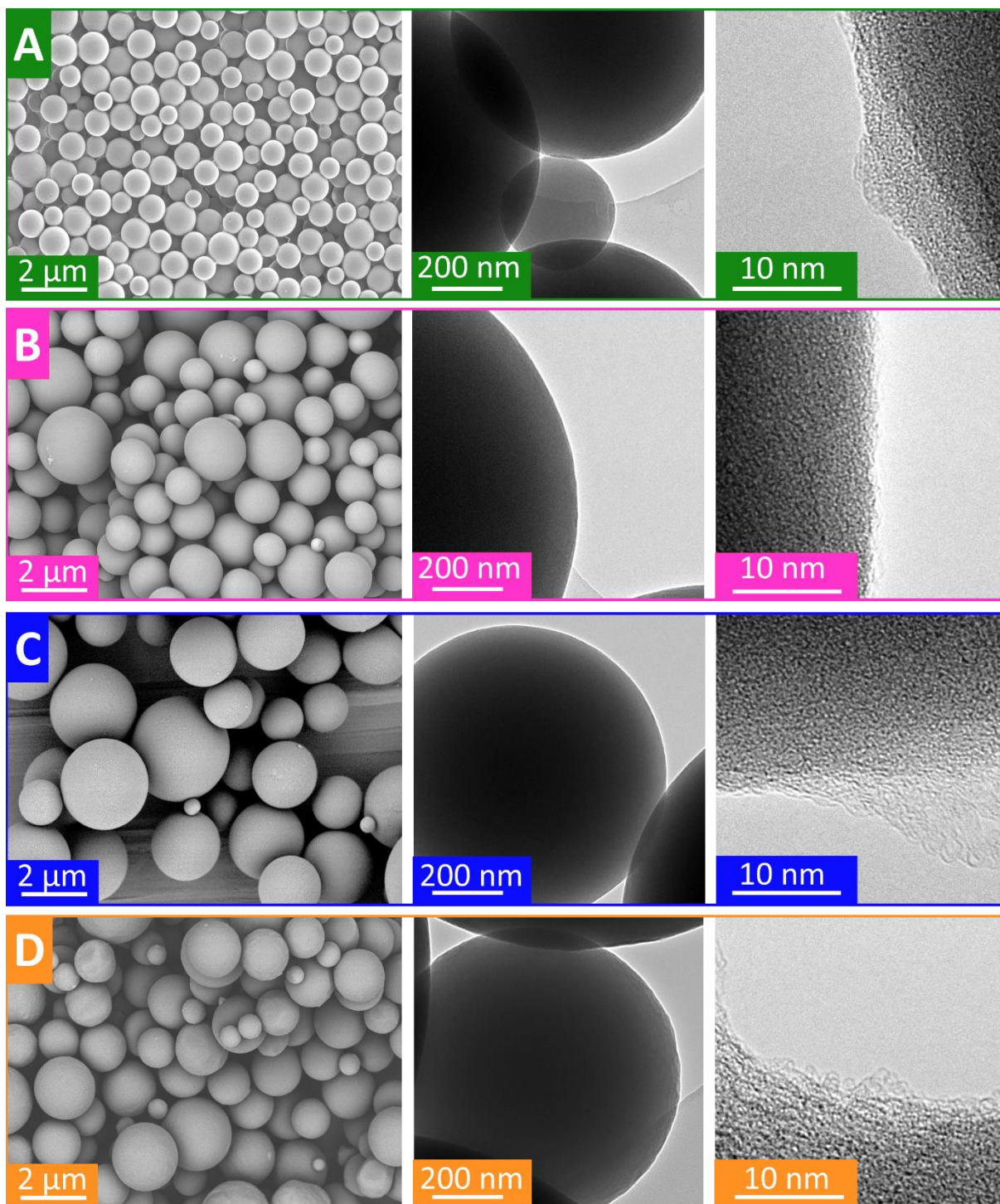


Figure S2: Scanning and transmission electron micrographs of the polymer beads Vi-SiO_{1.5} (A), Ph_{0.25}Vi_{0.75}-SiO_{1.5} (B), Ph_{0.5}Vi_{0.5}-SiO_{1.5} (C), and Ph_{0.75}Vi_{0.25}-SiO_{1.5} (D).

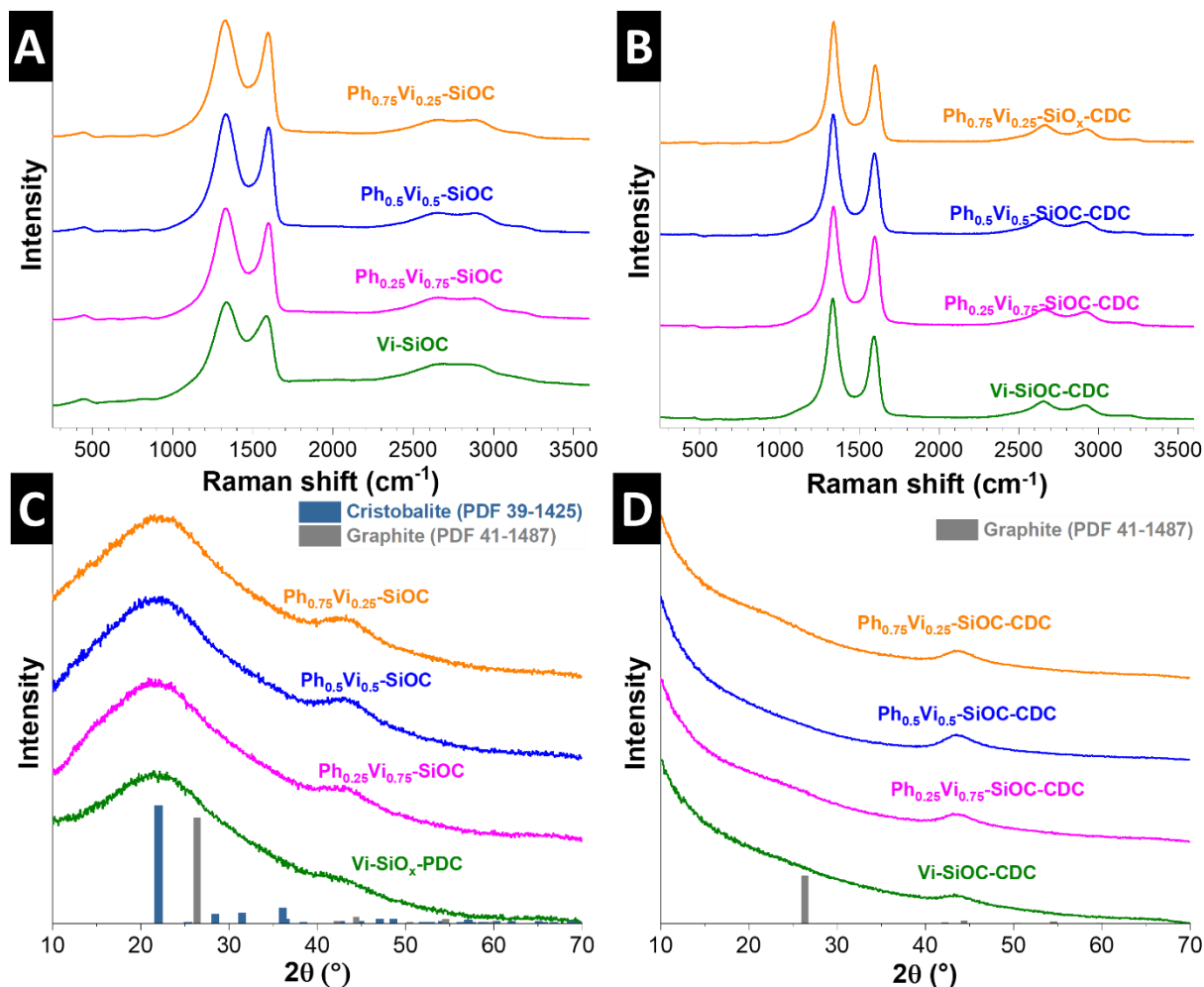


Figure S3: Raman spectra of PDCs (A) and CDCs (B). XRD pattern of PDCs (C) and CDCs (D).

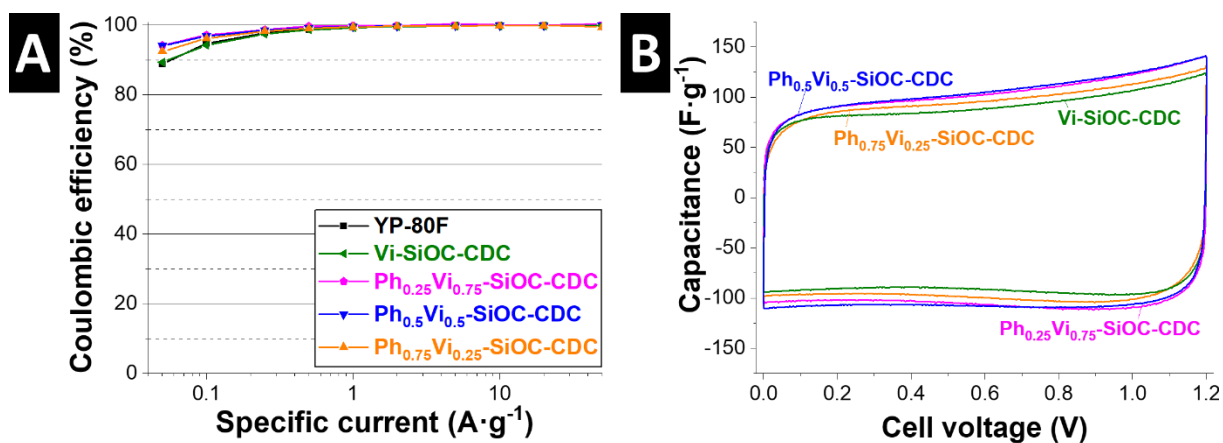


Figure S4: Coulombic efficiencies of all CDC materials including the AC in TEA-BF₄ in ACN (A) and cyclic voltammograms of all CDC samples in aqueous 1 M Na₂SO₄ (B) up to a cell voltage of 1.2 V.